European Journal of Pharmaceutical Sciences 213 (2025) 107249

Contents lists available at ScienceDirect

European Journal of Pharmaceutical Sciences

journal homepage: www.elsevier.com/locate/ejps

Designing fluorescent estrogen mimetic 7-hydroxycoumarin probe substrates for human sulfotransferase enzymes

Risto O. Juvonen [a,*], Pekka A. Postila [b,c,d,1], Pankaj Kumar Singh [b,c,1], Juhani Huuskonen [e], Juri Timonen [a], Muluneh Fashe [f], Rasikh Hussain [a], Zaeema Aqip [a], Olli Kärkkäinen [a], Hannu Raunio [a], Olli T. Pentikäinen [b,c,1]

[a] School of Pharmacy, Faculty of Health Sciences, University of Eastern Finland, Box 1627, FI-70211 Kuopio, Finland
[b] Institute of Biomedicine, Faculty of Medicine, University of Turku, FI-20014 University of Turku, Finland
[c] InFLAMES Research Flagship Center, University of Turku, FI-20014 Turku, Finland
[d] Neuronal Signalling Laboratory and Turku Screening Unit, Turku Bioscience Centre, University of Turku and Åbo Akademi University, Turku, Finland
[e] University of Jyvaskyla, Department of Chemistry, P.O. Box 35, FI-40014 University of Jyvaskyla, Finland
[f] Division of Pharmacotherapy and Experimental Therapeutics, Unc Eshelman School of Pharmacy, University of North Carolina at Chapel Hill, Chapel Hill, NC, USA

ARTICLE INFO

Keywords:
Human
Estrogen
Structure-activity relationship (SAR)
7-hydroxycoumarin
Active site
Sulfotransferase (SULT)

ABSTRACT

Sulfonation is one of drug metabolism reactions affecting homeostasis of estrogens. C-3 aryl substituted 7-hydroxycoumarins are fluorescent estrogen mimetics; i.e., the hydroxyl groups of both estrogens and 7-hydroxycoumarins are conjugated by human sulfotransferases (SULTs). Sulfonation of the 7-hydroxyl group by SULTs decreases the fluorescence of 7-hydroxycoumarins. Sulfonation of a series of 7-hydroxycoumarins by human SULTs was determined based on this property. SULT subtype-specific binding interactions of 7-hydrocoumarins were assessed against the modelled optimal arrangement needed for sulfonation. 3-(4-Methoxyphenyl)-7-hydroxycoumarin (**11**) and 3-(4-hydroxyphenyl)-7-hydroxycoumarin (**9**) were selective substrates for SULT1E1, whereas 3-(1H-1,2,4-triazol-1-yl)-7-hydroxycoumarin (**14**) was a selective SULT1A1 substrate. Other tested 7-hydroxycoumarin were sulfonated by more than two SULTs. Sulfonation of most 7-hydroxycoumarins by SULT1A1 or SULT1C4 followed Michaelis-Menten kinetics, while substrate inhibition kinetics occurred in sulfonation of several derivatives by SULT1E1. Selective sulfonation of derivatives **9** and **11** by SULT1E1 was due to the enzyme's long and cylindrical active site that assures optimal 7-hydroxyl group placement in the precursory reaction state. SULT1A1 and SULT1C4 preferred smaller derivatives as substrates than the SULT1E. Estrogens potently inhibited the sulfonation of 3,4-dimethyl-7-hydroxycoumarin (**4**) by SULT1E1 (IC_{50} below 1 μM). SULT1A1 and SULT1C4 were less potently inhibited by the estrogens. Several 7-hydroxycoumarin derivatives share common binding interaction patterns with the estrogens at SULT1E1 and SULT1A1 active sites. Fluorescent 7-hydroxycoumarins could serve as convenient probe substrates for SULTs to evaluate their inhibition by new chemical entities during drug development. 7-Hydroxycoumarins **9** or **11** could be used as selective probe substrates for SULT1E1 and **14** for SULT1A1.

1. Introduction

Estrogens regulate many key functions of the mammalian body, such as reproduction, anabolic functions, immune defense, and function of several organs such as the brain and bone via binding to estrogen receptor (ER) α or β (Amenyogbe et al., 2020; Gibson et al., 2020). In humans, the three most important active estrogens are estradiol (Fig. 1A–D) estrone, and estriol (Thomas and Potter, 2013). Estradiol is the most abundant estrogen in the blood during reproductive years, estrone is predominant during menopause, and estriol levels increase specifically during pregnancy. On one hand, estrogen derivatives are widely used for contraception and menopausal hormone replacement therapy in women (Levin et al., 2017). On the other hand, estrogen-dependent cancers are treated with ER antagonists or

* Corresponding author at: School of Pharmacy, Faculty of Health Sciences, University of Eastern Finland, Box 1627, FI-70211 Kuopio, Finland.
E-mail address: risto.juvonen@uef.fi (R.O. Juvonen).
[1] Permanent address: Institute of Biomedicine, Faculty of Medicine, University of Turku, FI-20014 University of Turku, Finland.

https://doi.org/10.1016/j.ejps.2025.107249
Received 11 June 2025; Received in revised form 26 August 2025; Accepted 28 August 2025
Available online 28 August 2025

inhibitors preventing estrogen synthesis (Isaacs et al., 2017).

Homeostasis of estrogens is the balance between their synthesis and metabolism. Estrogens are metabolized via oxidation by CYP (cytochrome P450) enzymes, via reduction by steroid dehydrogenases, and via conjugation by UGT (uridine 5′-diphospho-glucuronosyltransferase), SULT (sulfotransferase; Fig. 1A and B), or COMT (catechol-O-methyltransferase) enzymes. Sulfonation of estrogens by SULTs (Fig. 1D) – the transfer of the sulfonate group from the 3′-phosphoadenosine 5′-phosphosulfate (PAPS) to the OH group – has a special role in the homeostasis as the generated conjugates do not bind to ERs (Amenyogbe et al., 2020; Gibson et al., 2020). Instead, the sulfonated conjugates act as estrogen storage in the blood from where they are transferred to target tissues by influx transporters. Ultimately, active hormones are re-released to bind to ERs via hydrolysis by sulfatase enzymes (Thomas and Potter, 2013; Yi et al., 2021). Consequently, back-and-forth sulfonation and de-sulfonation play an important role in the estrogen homeostasis (Jiang et al., 2016).

Cytosolic SULTs, including several members of sub-subclasses of E.C. 2.8.2., catalyze sulfonation reactions of xenobiotics and endogenous substances, such as estrogens (Blanchard et al., 2004; Testa and Krämer, 2008; Parkinson et al., 2019). SULTs sulfonate small lipophilic alcohols, phenols, hydroxyamines or amine xenobiotics to more hydrophilic sulfate or sulfamate metabolites. When the sulfonate group is transferred from the cofactor PAPS to these compounds, simultaneously, adenosine 3′,5′-biphosphate (PAP) is released in the sulfonation conjugation (Fig. 1D and 1G). Humans express altogether 14 SULT forms, of which SULT1 and SULT2 families are responsible for the catalysis of xenobiotics (Coughtrie, 2016). SULT1E1 is the most important subtype in converting estradiol, estrone, and estriol to their sulfate conjugates, however, SULT1A1 (Fig. 1A and B) contributes as well (Yi et al., 2021).

Coumarin provides excellent scaffold for probing estrogen-related drug targets. We have previously presented 3-phenyl-coumarin analogs that bind to ER-α (Niinivehmas et al., 2016) or block estradiol synthesis by inhibiting 17-β-hydroxysteroid dehydrogenase 1 (17HSD1) (Niinivehmas et al., 2018). In addition, 3-imidazole-coumarin was identified as a potent aromatase (CYP19A1) inhibitor, demonstrating that the coumarin core can be tailored with specific ring and polar moiety substitutions to block different steps of estradiol synthesis (Niinivehmas et al., 2018; Niinivehmas and Pentikäinen, 2021). Estrogens and 3-phenyl-coumarin analogs share common structural features. The dimensions are similar depending on substituents in the 3-phenyl ring of coumarin analogs. Also, other topological features can be highly similar, for example, 3-(4-hydroxyphenyl)-7-hydroxycoumarin is similar to estradiol in that the distance between two OH groups and the volume of the molecules are equivalent and, importantly, both molecules contain a OH group that can be sulfonated. Notably, 3-cyano-7-hydroxycoumarin has been co-crystallized with SULT1A1 (Fig. 1E and F), which suggests that 7-hydroxycoumarin is also a suitable scaffold for

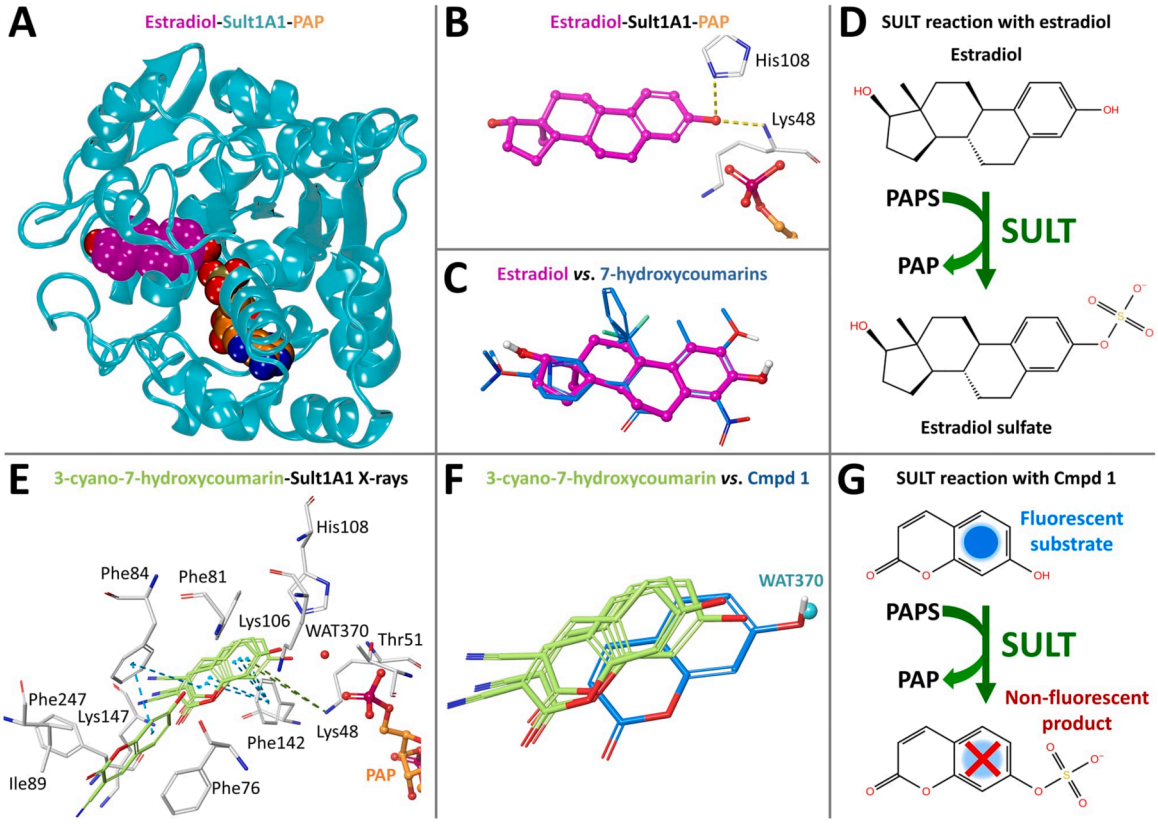

Fig. 1. Sulfonation of estradiol and 7-hydroxycoumarin occur similarly in the active site of sulfotransferases. A) The estradiol-SULT1A1 X-ray crystal structure with the depleted cofactor 3′-phosphoadenosine 5′-phosphosulfate or PAP (PDB: 2D06 (Gamage et al., 2005); B chain) is shown using CPK models and cyan cartoon. B) Zoom in, the SULT1A1-estradiol complex with the 7-OH group's key interaction partners at the catalytic end of the active site. C) The overlap of 19 7-hydroxycoumarin derivatives (blue stick models) is shown against the protonated estradiol (pink ball-and-stick model). D) SULT1E1 and SULT1A1 catalyze transfer of sulfone from PAPS to hydroxyl (or OH) group of estradiol, when the estradiol sulfate is formed. E) Three co-crystallized 3-cyano-7-hydroxycoumarins (green stick models; PDB: 3U3O, 3QVV, 3U3M (Berger et al., 2011)) are shown against the PAP-SULT1A1 complex structure to indicate that the canonical coumarin ring orientation is roughly similar to the pre-reaction alignment modelled for the new 7-hydroxycoumarin derivatives. F) Zoom-in, the co-crystallized 7-hydroxycoumarins and the canonical placement are shown without protein residues. The 7-OH is placed at the same site as co-crystallized water (WAT370). G) The sulfonation reaction of 7-hydroxycoumarins (shown with **1**) deletes the compounds' fluorescence. The π-π interactions (cyan) and potential hydrogen bonds or H-bonds (yellow; only panel B) are shown with dotted lines. The amino acid residues lining the active sites are shown with white stick models. For clarity, only polar hydrogen atoms are shown.

targeting SULTs.

The regulation of estrogen homeostasis is dependent on the balance between the substrate synthesis and their metabolism to inactive metabolites (Fig. 1D), the release of sulfate conjugates, and direct excretion (Thomas and Potter, 2013; Yi et al., 2021; Jiang et al., 2016). SULT1E1 and SULT1A1 have a dual role in estrogen homeostasis because they transform active estrogens to excretable or inactive storage forms as sulfate conjugates (Fig. 1D) (Yi et al., 2021). In target tissues, estrogens are released from the storage sulfate conjugates by sulfatase enzymes (Reed et al., 2005). Estrogen sulfonation by SULT1E1 and SULT1A1 can be measured by incubating estrogens either with tissue samples (e.g., liver) or recombinant SULTs. Next, the sulfate metabolites and parent substrates are separated, for example using high-performance liquid chromatography (LC) and quantified using a suitable detector system such as mass spectrometry (MS) using standards (Kushida et al., 2011; Ledeck et al., 2022). Although reliable, this assay is a very demanding and time-consuming procedure when estrogen substrates are used.

Therefore, it would be highly beneficial if inexpensive and easy-to-use assays were available to measure the enzymatic activity of all partners involved in these processes. To remedy this issue, we present here convenient and robust assays for probing SULT1A1 and SULT1E1 activity using fluorescence or absorbance-based 7-hydroxycoumarin substrates (Fig. 1G) instead of relying on estrogens. The applied fluorescence-based method was used to determine the sulfonation activity of thirteen 7-hydroxycoumarins (Figs. 1C and S1) and compared their hepatic sulfonation in vitro between human and six animal species in a prior study (Juvonen et al., 2020), however, the human SULT subtype selectivity of 7-hydroxycoumarins has not been tested previously.

The main objectives of this study were 1) to evaluate the selectivity of 7-hydroxycoumarins on eight human SULTs, focusing especially on estrogen sulfonating SULT1A1 (Fig. 1A-B) and SULT1E1, and, 2) to identify novel fluorescent 7-hydroxycoumarin-based substrates for these subtypes (Fig. 1G). SULT selectivity and enzyme kinetics were determined using a fluorometric assay (Juvonen et al., 2020) or a comprehensive series (N = 19) of existing and newly synthesized 7-hydroxycoumarin derivatives (Fig. S1). Molecular modeling and structural bioinformatics were applied to explain the activity and selectivity differences for the derivatives with the human SULTs. The results demonstrate that 1) there are many similarities in the binding of estradiol and 7-hydroxycoumarins to the catalytic cavities of SULT1E1 and SULT1A1; 2) There is a clear overlap between the SULT forms sulfonating 7-hydroxycoumarins and estrogens; and, 3) most importantly, it is demonstrated that 7-hydroxycoumarin scaffold can be tailored to function as selective probe substrate for the estrogen sulfonating SULTs.

2. Materials and methods

2.1. Experimental methods

Chemicals. PAPS, 7-hydroxycoumarin (umbelliferone, **1**) (99 %), 7-hydroxy-4-trifluoromethylcoumarin (HFC, **2**) (99 %), 6-methoxy-7-hydroxycoumarin (scopoletin, **3**), 17beta-estradiol (estradiol), estrone and estriol were procured from Sigma-Aldrich (Mannheim, Germany). $MgCl_2$ was procured from Riedel-de Haen (Vantaa, Finland). Water was deionized by MilliQ gradient A10. The 7-hydroxycoumarin derivatives 3,4-dimethyl-7-hydroxycoumarin (**4**), 3-ethyl-4-methyl-7-hydroxycoumarin (**5**), 3-ethyl-4,8-dimethyl-7-hydroxycoumarin (**6**), 3,4,8–trimethyl-7-hydroxycoumarin (**7**), 3-(4-methylphenyl)-7-hydroxycoumarin (**8**), 3-(4-hydroxyphenyl)-7-hydroxycoumarin (**9**), 3-(4-fluorophenyl)-7-hydroxycoumarin (**10**), 3-(4-methoxyphenyl)-7-hydroxycoumarin (**11**), 3-(4-dimethylaminophenyl)-7-hydroxycoumarin (**12**), 3-(4-pyridin-3-yl)-7-hydroxycoumarin (**13**), 3-(1H-1, 2, 4-triazol-1-yl)-7-hydroxycoumarin (**14**), 4-isopropyl-5-methyl-7-hydroxycoumarin (**15**), 4-phenyl-7-hydroxycoumarin (**16**), 4-phenyl-8-methyl-7-hydroxycoumarin (**17**), and 4-methyl-8-nitro-7-hydroxycoumarin (**18**) were synthesized using the Perkin-Oglialor condensation reaction or von Pechmann condensation reaction described in detail earlier (Timonen et al., 2011; Juvonen et al., 2018). Structures of 8–14 were confirmed by 1H-, 13C—NMR, ESI-MS (or HRMS), and elemental analysis (Niinivehmas et al., 2016; Juvonen et al., 2018).

The structures of 7-hydroxycoumarin derivatives are shown in Fig. S1.

Recombinant human SULT enzymes. *Escherichia coli* expressed human SULTs 1A1×1 (1A1), 1A2, 1A3, 1B1, 1C2, 1C4, 1E1, and 2A1 were purchased from CYPEX (Dundee, Scotland, UK) and stored at −80 °C in small aliquots.

Sulfonation assay. Reaction mixtures for sulfonation assays contained 100 mM potassium phosphate buffer pH 7.4, 2.5 mM $MgCl_2$, 10 μM PAPS, 0.05–0.3 g/L SULT as enzyme source and 10 μM 7-hydroxycoumarin derivative as substrate in the screening experiment or 0–20 μM in the kinetic experiments. 7-Hydroxycoumarin was dissolved in dimethyl sulfoxide, whose maximum concentration was 1 % in the assays. Negative control mixtures were performed without the substrate, the cofactor PAPS, or the enzyme source. Incubations were carried out in a 96 multi-well plate format in 100 μl volume at 37 °C. Fluorescence decline of the substrates was monitored every other minute for 40 min after the addition of PAPS, using an excitation filter at 405 nm and detection at 460 nm, in a Victor2 1420 Multilabel counter (PerkinElmer, Life Sciences, Turku, Finland). Fluorescence values were transformed to molarity using the substrates to create standard curves at every time point. Slopes of the decrease in substrate concentration per minute were calculated using linear regression analysis, in which the slope of the linear part of the kinetic assay indicated the sulfonation rate (μM/min). The sulfonation rate was calculated by subtracting the blank slope value from the full reaction value and normalizing the sulfonation rate by the protein concentration.

Enzyme kinetic analyses were performed in the same 96 multi-well plate assays, with excitation at 405 nm and detection at 460 nm, using different substrate concentrations (0–20 μM) and low concentrations of SULT enzymes so that the reaction rate could be calculated from the linear phase of the incubation. The kinetics of Michaelis and Menten and substrate inhibition kinetics were analyzed using equations $v = S * V_{max}/(K_m + S)$ and $v = S * V_{max}/(K_m + S * (1 + S/K_i))$, respectively. Symbols of these equations are v is the reaction rate, S substrate concentration, V_{max} limiting the rate of the reaction, K_m Michaelis-Menten constant equal to the substrate concentration, at which the reaction rate is 50 % of V_{max}, and K_i inhibitor constant (Leow and Chan, 2019). Excel and GraphPad Prism5 programs were used to analyze data and to draw graphs.

In the inhibition of sulfonation of derivative **4** by estrogens, estradiol, estrone or estriol concentration varied 0.128–200 μM estrogens at 100 mM phosphate pH 7.4 containing 5 mM $MgCl_2$, 10 mg/L SULT, 10 μM PAPS and 4 μM (SULT1A1), 2.5 μM (SULT1C4) or 7 μM (SULT1E1) compound **4**. Slopes (μM/min) of the decrease in substrate concentration per minute were calculated using linear regression analysis without inhibiting estrogen and at every inhibitor concentration. After subtracting the negative control slope, the relative remaining activity (v_i/v_0) was calculated by dividing the slope at inhibitor concentration by the slope without inhibitor. The IC_{50} value (inhibitor concentration decreasing activity by 50 %) was calculated using the equation $v_i/v_0 = 1/(1+IC_{50}/I)$, in which I was inhibitor concentration.

Multivariate analysis. The principal component analysis (PCA; Fig. S3) was performed using SIMCA 15.0.2 (Umetrics). For analysis of 7-hydroxycoumarin derivatives sulfonation at 10 μM concentration by eight human SULTs, we first normalized the values within samples from the sulfonation of the same substrate so that all values were divided by the highest value (normalized value = value / max value), due to the large variation in sulfonation rate between samples from different SULTs.

2.2. Computational methods

Precursory reaction state. The precursory state for sulfate transfer was modelled for the estradiol-PAPS-SULT1A1 complex (Fig. 2A) using MAESTRO (Schrödinger Release 2022–3; Schrödinger, LLC, New York, NY, 2018) based on the equivalent X-ray crystal structure with the depleted cofactor PAP (PDB: 2D06; B chain) (Gamage et al., 2005). The terminal SO3 group was 3D sketched and minimized directly into the active site, and then, the system protonation was set to match pH 7.4 ± 0.0 using PROPKA, and added hydrogens were optimized with the OPLS4 (Optimized Potentials for Liquid Simulations) force field (Lu et al., 2021) in the Protein Preparation Workflow. Finally, the entire system was minimized using the solvation model VSGB and OPLS4 force field using the default settings of PRIME (Jacobson et al., 2004).

Ligand preparation and pK_a analysis. The 3D structures of derivatives were drawn in 3D in MAESTRO and processed with LIGPREP with OPLS4 charges at pH 7.4 ± 0.0. Notably, the C7-phenol of **18** was deprotonated and negatively charged based on the employed EPIK prediction (Shelley et al., 2007). Accordingly, further computational pK_a titration analysis was performed with MARVIN22.18.0 (ChemAxon; https://www.chemaxon.com) to acquire additional confirmation for the result. Given that the deprotonated C7-phenol is right next to the C8-nitro group, the in silico result is logical and plausible; but no experimental effort to verify the predictions was invested due to the inactivity of the compound in the assay. The rest of the derivatives were predicted to be protonated, as shown in their 2D representations (Fig. S1).

Protein structure and ligand alignment. All of the human SULTs 1A1, 1A2, 1A3, 1B1, 1C1, 1C4, 1E1, and 2A1 X-ray crystal structures were acquired from the Protein Data Bank (PDB) (Berman et al., 2000) and, likewise, their representative AlphaFold Database (Jumper et al., 2021) models were downloaded (02/17/2023) and aligned against the final SULT1A1 precursory reaction state model using the protein backbone Cα atoms with VERTAA in the BODIL Modelling Environment (Lehtonen et al., 2004). Moreover, the 7-hydroxycoumarin analogs were also aligned using the Ligand Alignment module in MAESTRO against the bound estradiol molecule to acquire the optimal C7-OH positioning that is required for the sulfate transfer activity. It is noteworthy that the 7-hydroxycoumarin binding could happen without the C7-OH acquiring the optimal catalysis position (Fig. 1E-F); however, in those cases, the activity would be lost, or if the coordination is infrequent due to unfavorable substrate-enzyme interactions, the activity would be significantly weakened. Lastly, for reference, the derivatives were also flexibly docked into the SULT1A1 model and the original PDB entry, where hydrogens were added with MAESTRO, using PLANTS1.2 with the ChemPLP scoring function (Korb et al., 2009). The bound estradiol coordinates were used as the docking centroid, and the search radius was set to 10 Å.

Figure preparation. MAESTRO was used to generate the 2D and 3D representations in the figures. For visualization purposes, the cofactor PAPS was added to the aligned SULT structures from the minimized estradiol-SULT1A1-PAPS model (Fig. 1A), which could be enhanced by protonation and default binding pose optimization in MAESTRO.

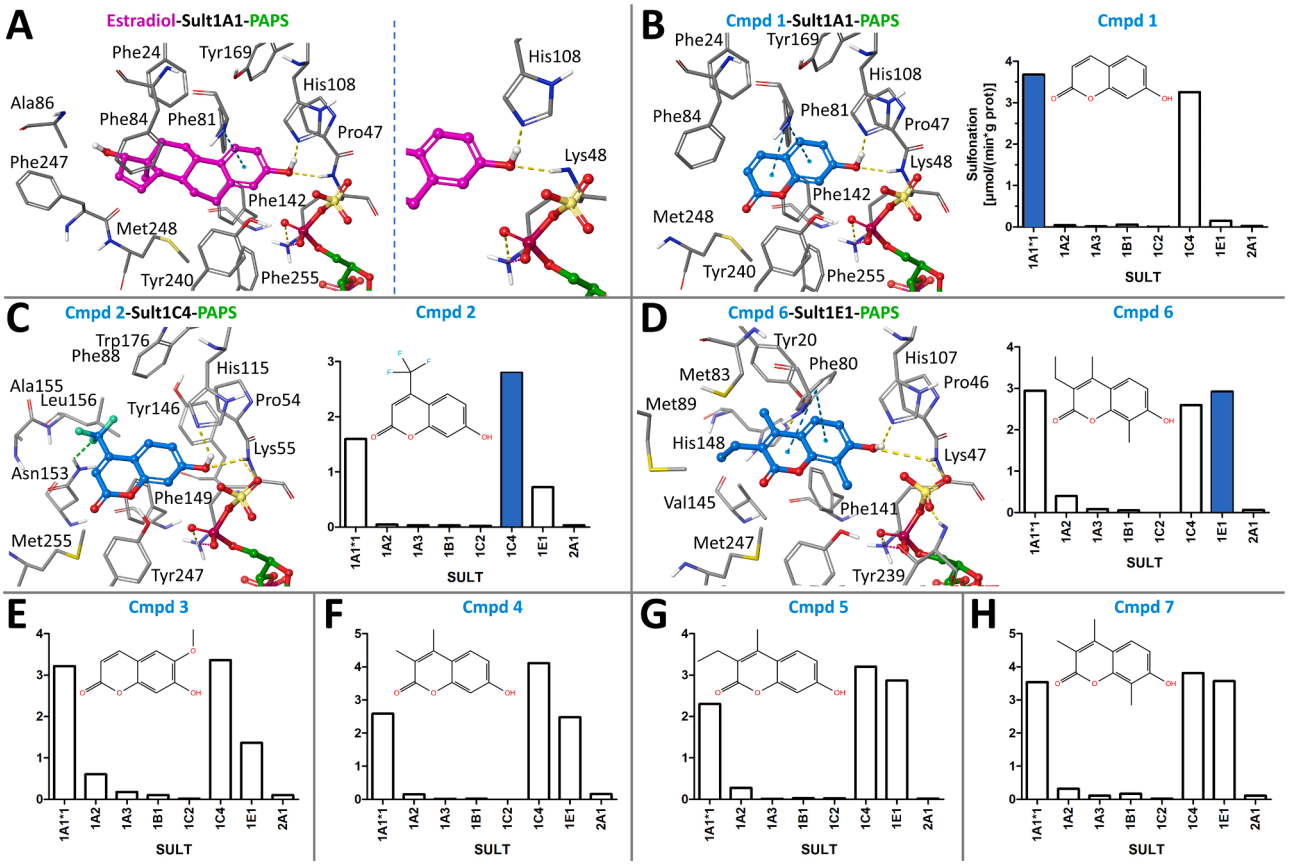

Fig. 2. Binding of selected group 1 7-hydroxycoumarins in the active sites of SULT1A1, 1C4 and 1E1 and sulfonation rates by eight human SULTs. The pre-reaction complex is shown for (A) estradiol-SULT1A1-PAPS complex (PDB: 2D06; B chain), (B) **1**-SULT1A1 complex (PDB: 2D06[6]), (C) **2**-SULT1C4 complex (PDB: 2GWH, chain A (Allali-Hassani et al., 2007)), and (D) **6**-SULT1E1 complex (PDB: 1G3M; A chain (Shevtsov et al., 2003)). The yellow dotted lines designate potential H-bonds, and the blue dotted lines show aromatic ring stacking. The sulfonation rates by different SULTs are shown with bar charts for derivatives B) **1**, C) **2**, D) **6**, E) **3**, F) **4**, G) **5**, and H) **7**. The ligand binding mode of **6** was optimized in MAESTRO for a better fit. The ionic bonds (magenta) are shown with dotted lines. The label of y-axis is the same in all bar charts (see panel B). For further information see Fig. 1 and Fig. S2.

3. Results

3.1. Precursory reaction model of SULT1A1 for optimal phenol placement prior to sulfate transfer

Firstly, the sulfonation rates of 19 derivatives of 7-hydroxycoumarin (Fig. S1) by human SULTs 1A1, 1A2, 1A3, 1B1, 1C2, 1C4, 1E1, and 2A1 were determined at 10 μM substrate concentration (Figs. 1G and S2; Table S1). Secondly, an optimal precursory reaction model for SULT1A1 was constructed with bound estradiol, where the transfer of sulfone group from the cofactor PAPS to the OH groups of estrogens or phenolic 7-hydroxycoumarin derivatives could happen (Fig. 1). PCA analysis was used to group the compounds according to their sulfonation rate and SULT selectivity (Fig. S3).

Several human sulfotransferase X-ray crystal structures exist in the PDB with either cofactor product PAP (SULT1A1 PDB: 2D06; SULT1E1 PDB: 4JVL) (Gosavi et al., 2013; Gamage et al., 2005; Pedersen et al., 2002) or phenolic substrate bound at the active site (Fig. 1E-F). There even exist SULT1E1 (PDB: 1HY3) and SULT2A1 (PDB: 4IFB) structures with bound cofactor PAPS 31]; however, due to the apparent reactivity and binding transiency, there are no crystal structures in which both the substrate and PAPS are present.

To understand better the binding of both the substrate and cofactor just before the sulfonation reaction takes place, the estradiol-PAPS complex was modeled by adding the terminal sulfonate (-SO_3) into the PAP molecule already present in the estradiol-SULT1A1 complex (PDB: 2D06 (Gamage et al., 2005); Fig. 1B vs. Fig. 2A). The modeled SO_3-terminus resides in a highly favorable niche for sulfonation, as it is stabilized by interactions with the nearby residues, and it bends toward OH-group of estradiol (Fig. 2A). This interaction takes place via hydrogen and ionic bonds in the active site, and the ester bond links SO_3 group to the 5′-phosphate group (Thomas and Potter, 2013). The C3-phenol of the substrate in the precursory estradiol-SULT1A1 model donates the H-bond to the His108 sidechain but, importantly, it also accepts an H-bond from the main chain nitrogen of Lys48 (or $Lys48^{NH}$; Fig. 2A).

3.2. Canonical 7-hydroxyl positioning of 7-hydroxycoumarin derivatives for sulfone transfer

The key reference point for analyzing the catalytic effectiveness or subtype selectivity of 7-hydroxycoumarin derivatives with the sulfotransferases is to focus on their C7-phenol's -OH occupancy at the above-mentioned catalytic position beside the sulfone group of PAPS in the eight SULT enzymes (Figs. 1F and 2A). To be sulfonated effectively 7-hydroxycoumarin derivatives need to acquire comparable -OH placement with estradiol. The substrate position at the catalytic site must be stabilized via interactions with amino acid residues to enable the OH sulfonation. For example, the binding mode of 7-hydroxycoumarins suggests that the coumarin ring's lactone oxygen atoms face a tyrosine sidechain (e.g., Tyr240 in SULT1A1 or Tyr239 in SULT1E1; Fig. 2B and D), where it interacts directly or via water. To support this, the water placement next to the tyrosine OH group, even with a bound ligand, is frequent in several SULT subtype structures (e.g., SULT1A1 PDB: 1LS6 (Gamage et al., 2003)) (Gamage et al., 2003). In addition, a similar but shifted canonical ring alignment is seen with the 3-cyano-7-hydroxycoumarin-SULT1A1 crystallized complexes (PDB: 3U3M, 3U3O, 3QVV; light green stick models in Fig. 1E-F) (Alcolombri et al., 2011; Berger et al., 2011).

The studied 7-hydroxycoumarins (Fig. S1) form three different groups based on their substitutions: (I) classical 7-hydroxycoumarins (derivatives **1**–**7**); (II) estrogen mimetics (derivatives **8**–**14**); and (III) new derivatives (derivatives **15**–**19**). Accordingly, different binding and sulfonation profiles were expected and quantified for them (Fig. S2; Table S1). A systematic structural comparison of human SULT X-ray crystal structures and pre-reaction state mimicking 7-hydroxycoumarin derivative superimposition was performed to explain the eight human SULT enzymes' catalytic differences generated by the different coumarin core substitutions. While alternative or low activity binding modes were also probed for SULT1A1 and other select derivative-SULT combination using flexible molecular docking, for clarity and brevity, the structure activity relationship (SAR) analysis focuses on the direct protein/ligand superimposition results rather than the varied binding predictions with no bearing on the activity results.

Group 1: Classical 7-hydroxycoumarins sulfonated by SULTs 1A1, 1C4, and 1E1

The 7-hydroxycoumarin derivatives **1**–**7** (Fig. S1 group 1), which lack substituents at the C3-position, present in derivatives **8–14** (Fig. S1 group 2), were sulfonated by SULT1A1, 1C4 and 1E1 (Figs. 2B-H and S2; Table S1), because they could adopt the canonical binding pose in these active sites. The orientation of 7-hydroxycoumarin scaffold pushes the C7-phenols of **1**–**7** beside the cofactor PAPS at the catalytic site. This phenol placement is aided by the favorable shape match with SULT1A1 cavity, and it is further stabilized by intra-protein H-bonds locking the compounds with Tyr169, Glu83, and His149. Substituents at the C4 and C5 positions improve the compounds' ability to fill favorably the cavity's hydrophobic sections, with the C3/C4-methyl groups of **4** and C4-dimethyl substituents of **5**, favoring interaction within the hydrophobic parts. The C6-methoxy group in **3**, which forms stabilizing interactions with Pro47 and Tyr169, further contributes to the effective substrate positioning. At the same time, the C8-methyl group in **6** enhances SULT1A1 sulfonation modestly by improving the positioning of the C7-OH for catalysis, as also indicated by its low K_m value (Table S2), likely displacing solvent molecules around the catalytic site.

SULT1C4 also demonstrated high sulfonation activity for derivatives **1**–**7** (Figs. 2B-H and S2; Table S1), whose smaller structures in comparison to the group 2 and 3 derivatives (Fig. S1) allow them to fit snugly within its compact catalytic site. C4-trifluoromethyl group of **2** (Fig. 2C), for instance, forms favorable interactions with $Asn153^{NH2}$, similar to known halogen placements in co-crystal structures like pentachlorophenol (PDB: 2GWH (Allali-Hassani et al., 2007)). In **3**, the interactions of the C6-methoxy group with Tyr140, Trp170, and Pro48 enhance sulfonate transfer activity, and with the C3/C4-methyl or C3-methyl/C4-ethyl groups additional stabilization is observed. This favorable binding is echoed across the analogs in this subset, with functional group placements effectively filling the active site.

SULT1E1 also demonstrated high sulfonation activity for derivatives **2**–**7** (e.g., **6** in Fig. 2D2 and S2; Table S1) and K_m-values of **3, 6,** and **7** are smaller than those of **2** and **4** (Table S2)**.** In contrast, the active site of SULT1E1, including Tyr20 near the catalytic end, presents a different binding environment than SULT1A1 or SULT1C4. Here, $Tyr20^{\circ H}$, H-bonded with His148, can stack with ligands, thus, potentially pulling the C7-phenol from its optimal catalytic placement, which in turn, reduces the sulfonation rate, as is seen with **1**. However, substituents like the C4-trifluoromethyl in **2** and C3/C4-methyl/ethyl additions in **4**–**7** compensate by anchoring the coumarin core, which restores or enhances the activity. For example, the C6-methoxy group in **3** (Fig. 2E) and the favorable cavity filling by the C8-methyl in **6** (Fig. 2D) improve C7-OH coordination, allowing activity comparable to or exceeding that observed with SULT1A1 and SULT1C4.

Group 2: Estrogen mimetics sulfonated mainly by SULT1E1

Derivatives **8**–**14** (Fig. S1) have a highly similar shape and size as well as phenol group placement to estradiol (e.g., **9** in Fig. 3C vs. Fig. 2A). Accordingly, it was expected that the 7-hydroxycoumarin derivatives of group 2 would also present similar binding modes and the sulfonation pattern as estrogens with SULT1A1 and SULT1E1. Indeed, with SULT1E1, all but **14** (Fig. 3H), which has a highly polar and slightly smaller substituent at C3-position than other group II derivatives, showed high sulfonation rates and low K_m-values (Figs. 3, S2, S4; Tables S1 and S2). However, the C3-positioned rings and varied substituents contributed significantly to sulfonation and distinct binding characteristics across the SULT subtypes, with particularly large

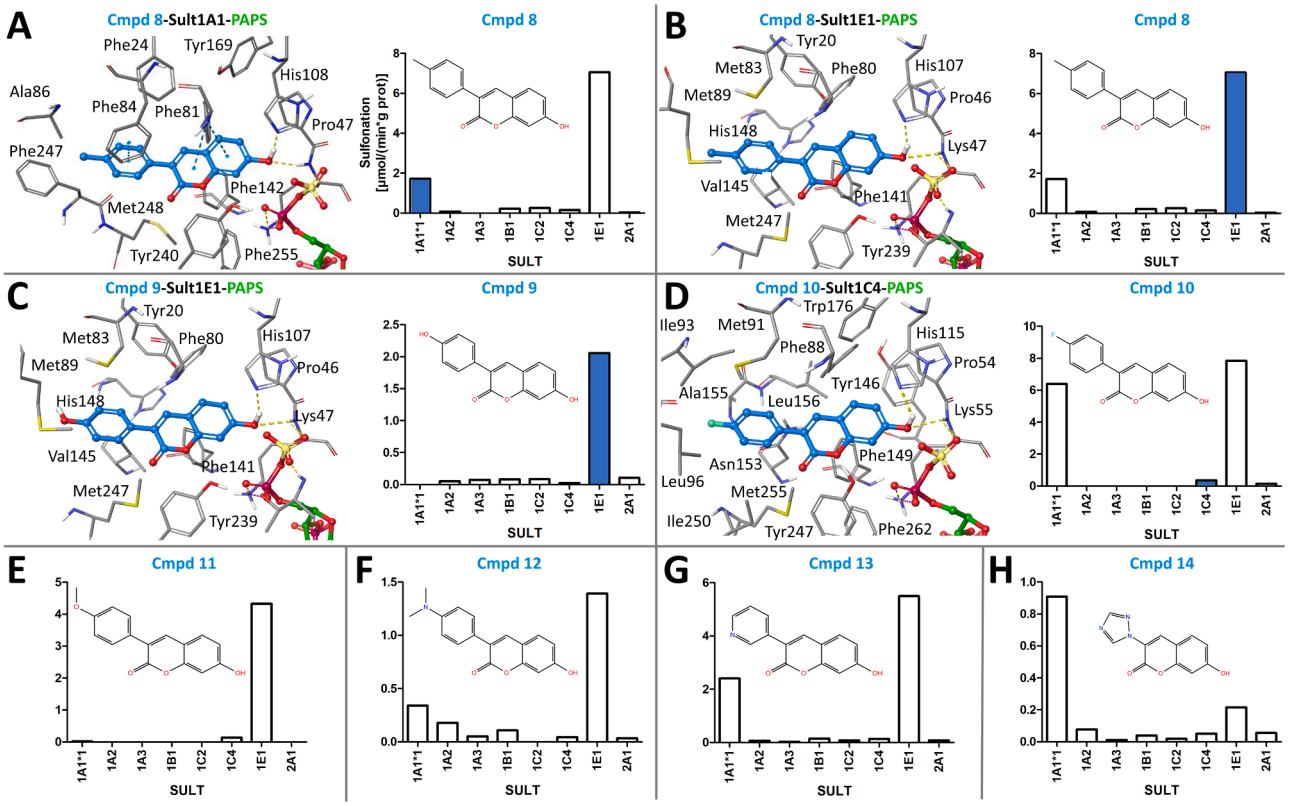

Fig. 3. Binding of selected group 2 7-hydroxycoumarins in the active sites of SULT1A1, 1C4 and 1E1 and sulfonation rates by eight human SULTs. The pre-reaction complex is shown for A) **8**-SULT1A1 (2D06; B chain (Gamage et al., 2005)), B) **8**-SULT1E1 (PDB: 1G3M; A chain (Shevtsov et al., 2003)), C) **9**-SULT1E1 (PDB: 1G3M; A chain (Shevtsov et al., 2003)), and D) **10**-SULT1C4 (PDB: 2GWH; chain A (Allali-Hassani et al., 2007)). The sulfonation rates by different SULTs are shown with bar charts for derivatives A) **8**, B) **6**, C) **9**, D) **10**, E) **11**, F) **12**, G) **13**, and H) **14**. The label of y-axis is the same in all bar charts (see panel A). For further information see Figs. 1–3.

variation with SULT1A1.

Derivatives **9** and **11** were sulfonated by SULT1E1 (Fig. 3C and E), but not by the other SULTs, being the most selective substrates for SULT1E1 (Fig. 3 and S2; Table S1). While **8**, with a C3-positioned 4′-methylphenyl, fits into active sites of SULT1E1 and shows high sulfonation rate (Figs. 3B and S2; Table S1), in the canonical pose it approaches the limits of the active site/cavity volume in SULT1A1 (Fig. 3A), which results in only a modest sulfonation rate (Fig. 3A, 3B and S2; Table S1). In **9**, there is a 4′-phenol C3-substituent present (Fig. 3C), leading to substantial similarity with estradiol, but surprisingly SULT1A1 does not sulfonate well its 7-OH-substituent. Sulfonation kinetics of **9** by SULT1E1 showed substrate inhibition (Table S2; Fig. S3). The 4′-phenol in **9**′s C3 substituent likely introduces polar interactions (Fig. 3C), allowing H-bonding with conserved water near Phe247° and Lys147^{NH}, potentially reversing the binding pose and reducing activity in SULT1A1, thus maintaining fluorescence due to the intact C7-OH.

C3-positioned 4′-fluorophenyl in **10** (Fig. 3D), smaller than the 4′-methylphenyl, generates high sulfonation rate, benefiting from favorable hydrophobic interactions with the cavity end residues of SULT1A1. In contrast, the 4′-methoxyphenyl of **11** (Fig. 3E) and the 4′-N,N-dimethylphenyl of **12** disrupt SULT1A1's sulfonation ability (Fig. 3F) due to their size and polarity interfering with optimal cavity filling. Derivative **13**, with a C3-pyrimidine ring (Fig. 3G), fits well into SULT1A1's non-catalytic end of the cavity but suffers reduced activity due to polar interactions between its ring nitrogen and the surrounding hydrophobic residues. Similarly, the C3-positioned 1,2,4-triazole ring in **14** (Fig. 3H) exhibits low activity in SULT1A1 due to its excessive polarity, making it an inefficient substrate. However, it is below 1 μM K_m (Table S2) and a selective substrate of SULT1A1 which was sulfonated with low rate by other SULTs. The broader cavity of SULT1E1 versus SULT1A1 can accommodate these compounds better, with derivatives like **13** benefiting from the more open binding pocket.

Group 3: C4-substituted derivatives sulfonated by several SULTs

The addition of C4-substitutions yielded varied sulfonation rates by several SULTs (Figs. 4 and S2; Table S1). The larger C4-substituents in **16** and **17** resulted in minimal sulfonation by SULT1A1 (Fig. 4C-D), likely because their bulky groups interfere with optimal positioning and prevent His149 sidechain adjustment. Coumarin co-crystal studies (e.g., 3-cyano-7-hydroxycoumarins in Fig. 1E-F) suggest that these derivatives could still bind to a secondary, non-catalytic site within SULT1A1.

With SULT1C4 and SULT1E1, however, **15**–**17** show a mixed pattern of sulfonation rates (Fig. 4B-D). The more open binding space of SULT1E1 permits the C4-phenyl of **17** or **18** to form π-π stacking with Tyr20 and Phe23, while the smaller 4-isopropyl of **16** is less efficient.

The lack of activity for **19** with all studied SULTs (Figs. 4E and S2) indicates that the presence of the C8-nitro (NO_2) group abolishes its sulfonation. From the structural perspective, the NO_2 group could take a similar position at the non-catalytic cavity end visible in the nitro-containing co-crystals (PDB: 1LS6, 3QVU, 3U3R) (Gamage et al., 2003; Alcolombri et al., 2011; Berger et al., 2011). From this location, the NO_2 group could, for example, H-bond with water, the Ser168$^{\circ H}$, and π-π stack with Phe24 in SULT1A1. This is possible because the NO_2 groups also tend to bind into hydrophobic and solvent-exposed cavities due to their "hydroneutral" profile (Sagawa and Shikata, 2014). When the protonation of **19** was studied at pH 7.4 using EPIK (Shelley et al., 2007) in the LIGPREP module of MAESTRO, it suggested that the C8-NO_2 group could deprotonate the C7-phenol. This was further validated with the in silico titration analysis with MARVIN, which indicates that 95.3 % of the group exist in the deprotonated form. Thus, even if **19** assumes the canonical pose, in which the NO_2 group could form π-cation

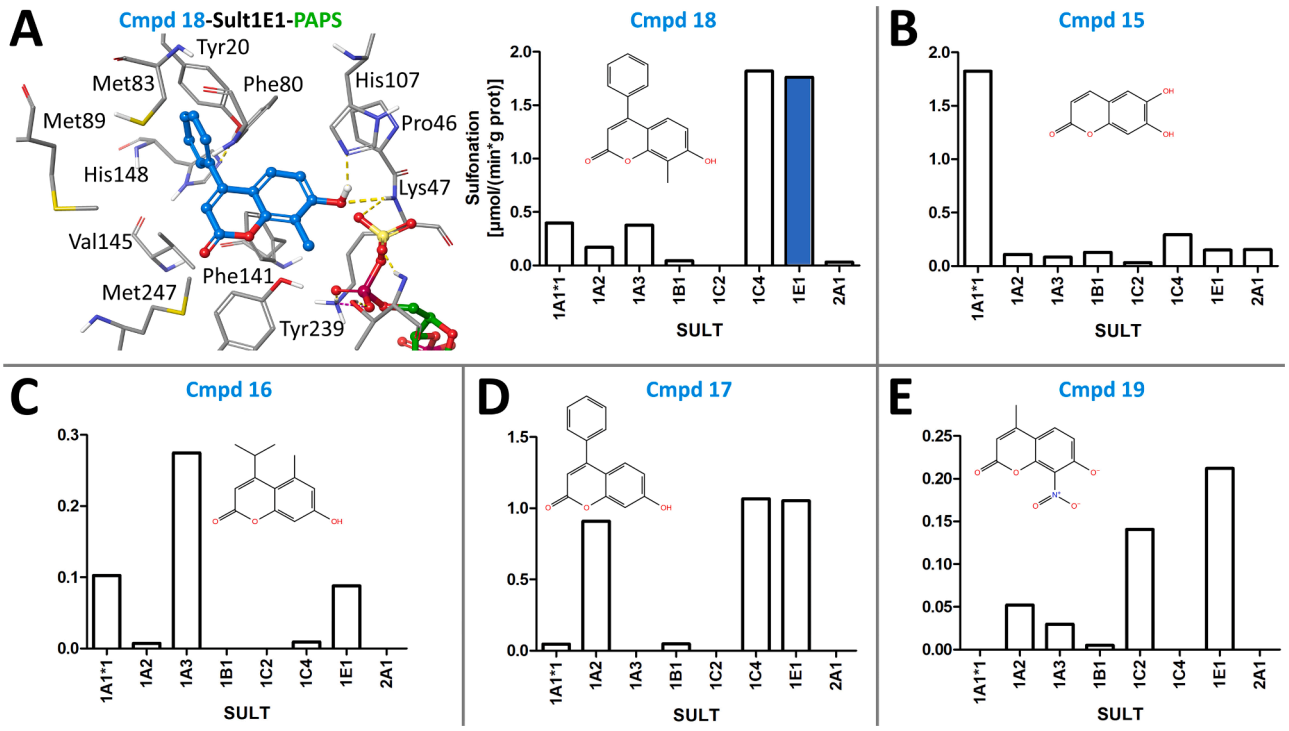

Fig. 4. Binding of derivative 18 in the active site of SULT1E1 and sulfonation rates of 7-hydroxycoumarins of group 3. A) The modelled pre-reaction state is shown for **18**-SULT1E1-PAPS complex (PDB: 1G3M; A chain (Shevtsov et al., 2003)). The sulfonation rates by different SULTs are shown with bar charts for derivatives A) **18**, B) **15**, C) **16**, D) **18**, and E) **19**. The label of y-axis is the same in all bar charts (see panel A). For further information see Figs. 2–3.

interactions with Phe142 and Tyr240, only shallow activity is seen because most of the phenol groups are likely deprotonated.

3.3. Explaining low sulfonation rates of 7-hydroxycoumarins by SULT1A2, 1A3, 1B1, 1C2, and 2A1

Sulfonation of all 7-hydroxycoumarin derivatives by SULT1A2, 1A3, 1B1, 1C2 and 2A1 were slower than by SULT1A1, 1C4 or 1E1 (Figs. 2–4 and S2; Table S1), and their docking and interactions with these enzymes are described in detail in the Supplementary Material (Fig. S6).

In SULT1A2, the small active site cavity volume (PDB: 1Z29; A chain) allows moderate activity for group III analogs such as derivative **17**, which packs its C4-phenyl into a hydrophobic pocket (Fig. S6A). However, the side chain of Ile21 overlaps with **17** assuming in the canonical pose, which highlights the difficulty for achieving suitable binding pose for the reaction. Additionally, the boundaries of the SULT1A2 cavity are impacted by the 4′-fluorophenyl of derivative **10** clashing with the phenyl ring of Phe247 at the non-catalytic end (Fig. S6B). In SULT1A3, an unmet negative charge at the non-catalytic cavity end, generated by the carboxylate groups of Glu146 and Asp86, cannot be utilized in the canonical binding mode by the analogs (e.g., 10 in Fig. S6C; PDB: 2A3R; A chain).

The SULT1B1 active site cavity contains Thr21, which H-bonds with the benzene-1.3-diol of resveratrol (PDB: 3CKL; Fig. S6D). Flexible molecular docking suggests that the 7-OH group of analogs like derivative **10** may also H-bond with the threonine sidechain, compromising the canonical positioning for optimal 7-OH placement. In SULT1C2, the positively charged Arg241 affects the positioning of 7-hydroxycoumarins at the enzyme's active site (Fig. S6E). Flexible docking of **1** suggested even a reversed docking pose where the 7-OH is completely opposite for the reaction to occur. Lastly, SULT2A1 favors flexible steroid conformations, as indicated by the binding pose of androsterone (PDB: 1OV4; A chain), which is not possible for the flat and straight 7-hydroxycoumarins (e.g., **10** in Fig. S6F).

3.4. Shape match between 7-hydroxycoumarins and SULT active site cavities explains sulfonation activity

The fitting of 7-hydroxycoumarins inside the active site cavities of eight SULTs differed greatly. This is illustrated for derivatives **1, 10**, and **18** inside the active sites of SULTs 1A1, 1C4, and 1E1 in Fig. 5. With SULT1A1, **1** fit well inside the active site, but the shape-fit was horizontally more complete for **10**, which, in turn, is reflected in its higher activity (Fig. 5A-B). Both the activity and shape fit are far worse for **18** as its C4-phenyl ring protrudes clearly out of the cavity in the canonical pose needed for the C17-OH sulfonation (Fig. 2). With SULT1C4, derivatives **1** and **18** have relatively good shape match with the cavity (Fig. 5C), but the fit is either slightly looser or tighter, respectively, than was the case with SULT1A1 (Fig. 5B) that also generated higher sulfonation rate (Fig. 5A). The phenyl ring of **10** is protruding out the SULT1C4 cavity and, while at first glance it looks similar to the other SULTs for its 4′-fluorophenyl placement (Fig. 5C vs. A-B), it actually overlaps with the side chain of Leu96 at the non-catalytic end. Moreover, with SULT1C4, the derivative's halogen is not facing positively charged lysine (not shown) unlike is the case with SULT1A1 (Lys86) or SULT1E1 (Lys85), which seems to lower markedly the activity of **10** (Fig. 5A). With SULT1E1, **10** provides excellent horizontal cavity fit reminding estradiol binding mode, which results in excellent activity in the fluorescence assay (Fig. 5A and D). In contrast, the SULT1E1 cavity is too large for **1** to fill the cavity's catalytic end stably and, while **18** seems to fit into the cavity, it is clearly not providing optimal match either vertically or horizontally. Interactions between ligands estradiol, **1** or **8** and SULT1A1, between ligands **2** or **10** and SULT1C4 and between ligands **6, 8, 9** or **18** and SULT1E1 are visualized with 2D representation in supplementary material (Fig. S7).

3.5. Probe substrate usage: In vitro inhibition of derivative 4 sulfonation by estrogens

Since SULT1A1 and SULT1E1 are known estrogen sulfonating

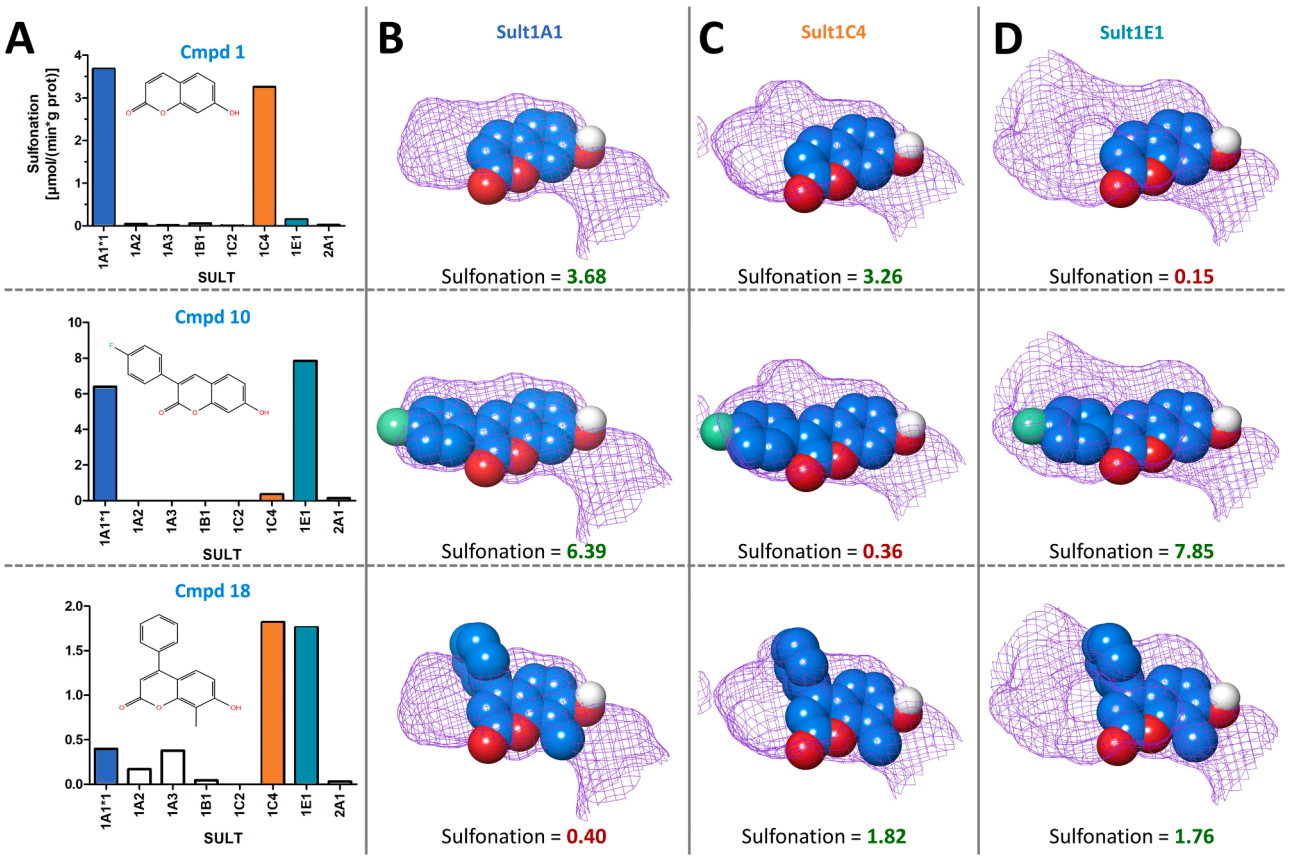

Fig. 5. Shape match between the 7-hydroxycoumarin derivatives and SULTs 1A1, 1C4, and 1E1 catalytic site cavities. A) The sulfonation rates (µmol/ (min* g prot) by eight SULTs are shown for one representative of each 7-hydroxycoumarin groups 1–3 or derivatives **1, 10**, and **18**, respectively (Fig. S1). Likewise, the shape fit between the active site cavity and **1, 10**, and **18** is shown for (B) SULT1A1, (C) SULT1C4, and (D) SULT1E1. The cavities available for binding of the substrates are shown using magenta mesh surfaces and the 7-hydroxycoumarins as blue CPK models. The label of y-axis is the same in all bar charts (see panel A). The sulfonation rates are provided numerically using red or green highlighting to indicate the lack of activity (≤1.00) or moderate/high activity (≥1.00), respectively.

enzymes, the ability of β-estradiol, estrone, and estriol to inhibit sulfonation of **4** by SULT1A1/SULT1C4/SULT1E1 at the K_m concentration was examined (Fig. 6). SULT1E1 was most potently inhibited (IC_{50} < 1 µM), followed by SULT1A1 (IC_{50} 2–5 µM for estradiol and estrone and 64 µM for estriol). SULT1C4 was not inhibited as the IC_{50} values were higher than 200 µM. These results show that **4** could be used as a tool compound to evaluate if a chemical compound, for example a drug candidate molecule in early development, inhibits SULT1A1, SULT1C4, and SULT1E1 and, therefore, potentially disturbs estrogen homeostasis.

4. Discussion

Sulfonation (Fig. 1D and G) is an important biotransformation pathway for the homeostasis of endogenous estrogens such as estradiol (Figs. 1A-C and 2A), estrone and estriol, because estrogen sulfates act as storage in blood circulation from where transporters transfer them to target organs and sulfatases release them to active forms in these organs (Thomas and Potter, 2013; Yi et al., 2021; Jiang et al., 2016). SULT1E1 is the major enzyme sulfonating estrogens in human, which are also sulfonated by SULT1A1[3,16].

In this study, the sulfonation of 19 7-hydroxycoumarin derivatives was quantified for eight human SULTs using a fluorometric assay (Juvonen et al., 2020). Due to the availability of a wealth of X-ray crystallographic data on the human SULTs (Gosavi et al., 2013; Gamage et al., 2005), a thorough structural bioinformatics analysis could be performed to explain the sulfonation rate differences between the 7-hydroxycoumarin derivatives and SULTs. Firstly, the precursory reaction model was generated for estradiol-SULT1A1 complex with the non-depleted cofactor PAPS (Fig. 2A). Secondly, this conserved arrangement for the natural estradiol substrate at the enzyme's active site, facilitating the optimal OH group placement for the sulfate transfer at the catalytic site (Fig. 1C and F), was utilized as a template in aligning or "docking" the 19 different 7-hydroxycoumarin derivatives (Fig. 1C). Thirdly, the other SULT subtype structures were aligned against this precursory SULT1A1 model to facilitate further binding or activity analysis via structural comparison (Figs. 2–4). This analysis is summarized for all derivatives and SULTs in a structure-sulfonation activity relationship or SAR model in Fig. 7.

Although the chemical structures of estrogens and 7-hydroxycoumarins are markedly different (Fig. 1C), their shape and size or volume roughly resemble especially with the 7-hydroxycoumarin derivatives having an aryl substituent at position 3 (Niinivehmas et al., 2018; Niinivehmas and Pentikäinen, 2021). Notably, these C3-substituted 7-hydroxycoumarins were found to be sulfonated by SULT1E1 or SULT1A1 (Fig. 3) and, additionally, several of the derivatives were found to be sulfonated by SULT1C4 (derivatives **2**–**7**; Fig. 2). However, based on molecular modelling, most of the 7-hydroxycoumarins were unable to establish the canonical pose at the active sites needed for the optimal 7-OH placement, resulting in the lack of sulfonation by the five remaining SULTs. Therefore, estrogens and aryl C3-substituted 7-hydroxycoumarin derivatives were sulfonated by the same human SULT enzymes such as SULT1E1 and SULT1A1. The most selective of these derivatives, **9** and **11,** are suitable to be used as fluorescent probe substrates to study estrogen sulfonating SULT1E1, and **14** for SULT1A1. Although not as optimal for assay usage, some of the less selective 7-hydroxycoumarin derivatives could also be used as

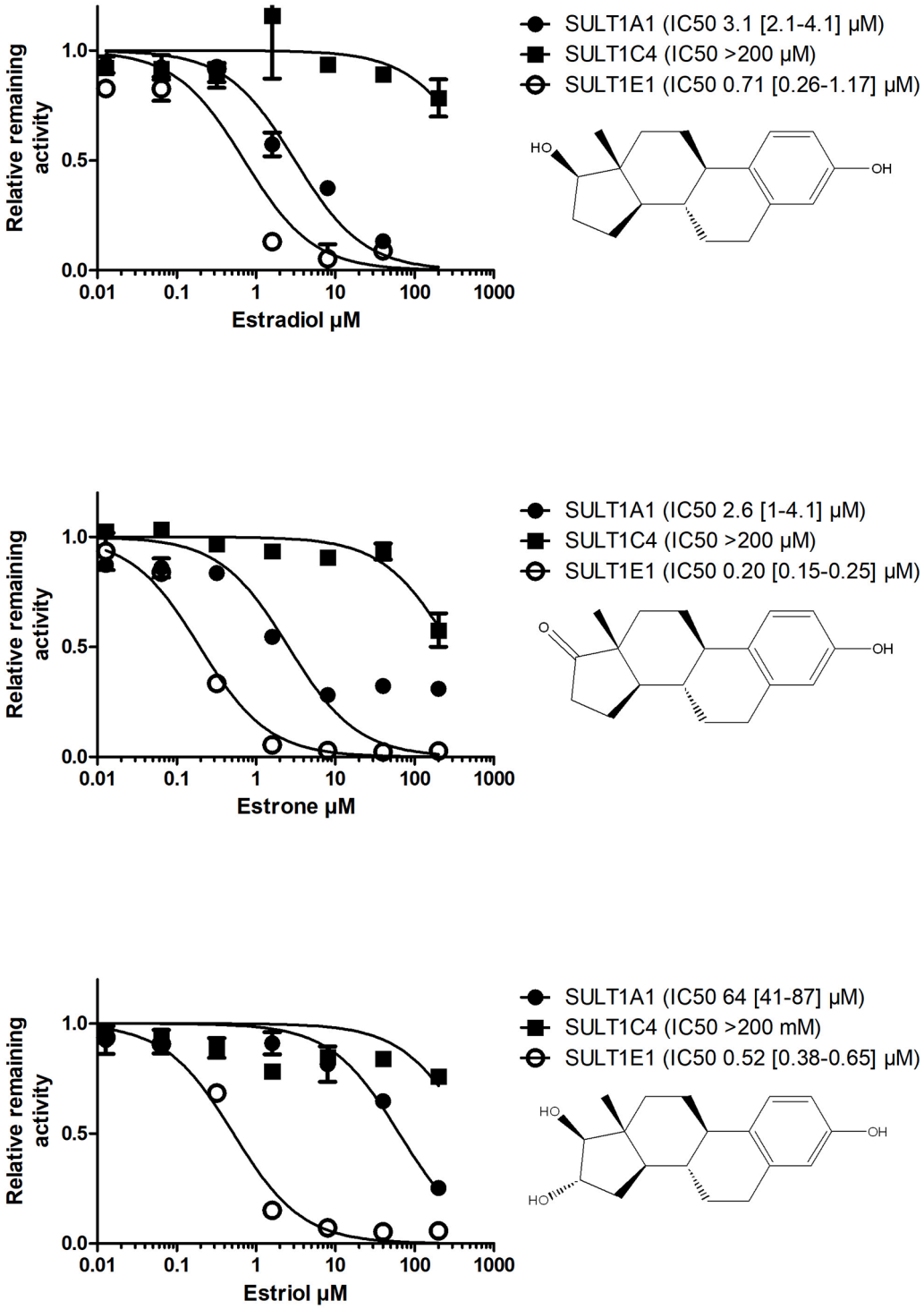

Fig. 6. Inhibition of SULTs 1A1, 1C4, and 1E1 catalyzed sulfonation of derivative 4 by β-estradiol, estrone, and estriol. Sulfonation of **4** was inhibited by 0.128–200 μM estrogens at 100 mM phosphate pH 7.4 containing 5 mM $MgCl_2$, 10 mg/L SULT, 10 μM PAPS, and **4** at concentrations of 4 μM (SULT1A1), 2.5 μM (SULT1C4), or 7 μM (SULT1E1) (Table S2). The relative remaining activity was calculated by dividing the inhibited activity by the activity without inhibitors. The average IC_{50} values of estrogens [95 % confidence limit] are given. Each point represents an average of two or three replicates.

fluorescent probe substrates for other SULTs in recombinant SULT assays, e.g., **7** for SULT1C4 and **18** for SULT1A2.

SULT1E1 is the major sulfotransferase of estrogens having low K_m-values of estrogens below μM (Yi et al., 2021; Nishiyama et al., 2002; Zhang et al., 1998). SULT1A1 supports significantly sulfonation of estrogens having higher K_m-values for estrogens above μM than SULT1E1 (Squirewell and Duffel, 2015). Estrogen mimetics **9** and **11** were selective SULT1E1 substrates, whereas **10**, and **13** were sulfonated by both SULT1A1 and SULT1E1. **14** was a rather selective substrate for SULT1A1. These 7-hydroxycoumarin derivatives fit well into the volumes of the active sites of these SULTs, which support the experimental finding about their sulfonation and kinetic parameters of the sulfonation reactions. K_m-values of **8**–**13** in SULT1E1 sulfonation were μM range, which is higher than the K_m-values of estrogens. Both 17β-estradiol and

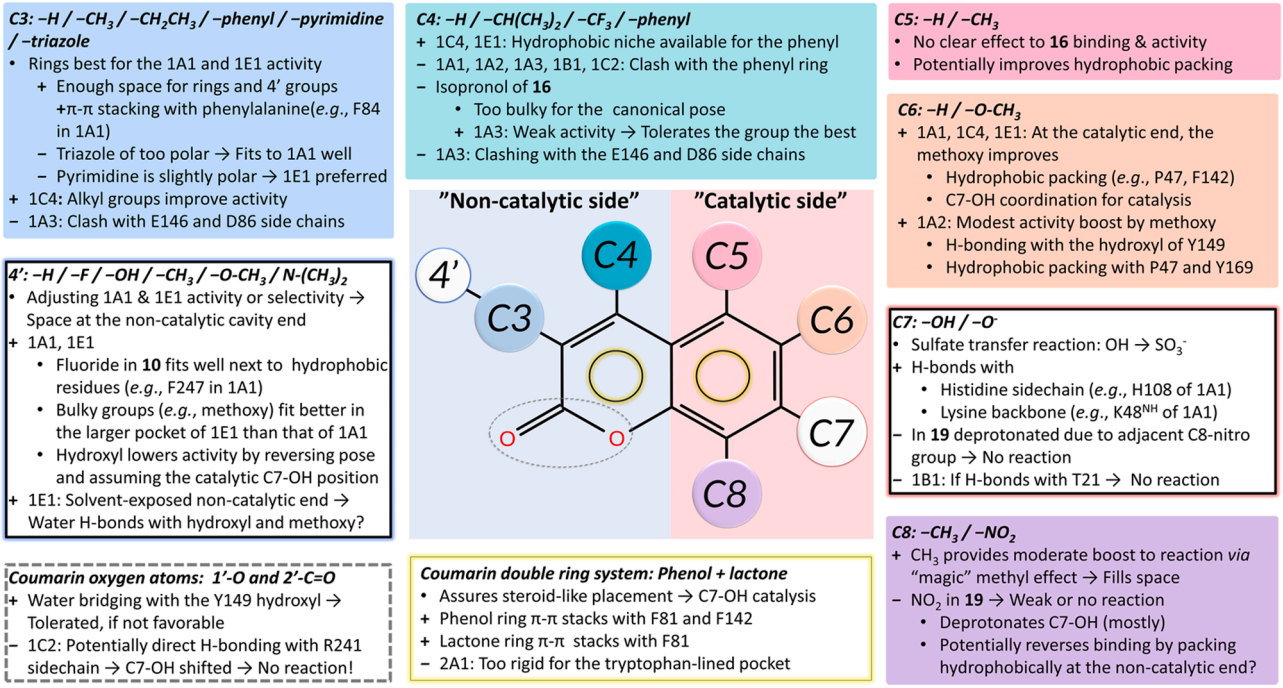

Fig. 7. Structure activity relationship analysis for sulfonation of 19 7-hydroxycoumarin derivatives by human SULTs. The SULT activity results (Fig. S2; Table S1) for the derivatives were compared against the backdrop of the SULT protein 3D structures via protein and substrate alignments or flexible docking.

8–**12** showed substrate inhibition in their sulfonation kinetics by SULT1E1 (Zhang et al. 1998). Compounds **8**–**14** mimic the structure of estrogens and both types of compounds are sulfonated by SULT1E1 and SULT1A1, into whose catalytic sites their OH group pose canonically for the sulfone transfer from PAPS. Characteristics of the active sites make it possible for both estrogens and derivatives **8**–**14** to fit in the canonical pose at the catalytic sites of SULT1E1.

Classical 7-hydroxycoumarins or derivatives **2**–**7** were sulfonated by both SULT1A1 and SULT1E1 (Fig. 2B-H) as was the case for **10, 13**, and **14** (Fig. 3D,G, and H), however, in addition they were also sulfonated by SULT1C4. Derivatives **1**–**7** could achieve suitable orientation in the catalytic sites of SULTs 1A1, 1C4, and 1E1 to be sulfonated, as they had smaller size than estrogen mimetic group 2 7-hydroxycoumarins (**8**–**14**) and aliphatic substitutions at positions 3, 4, 6 or 8 of coumarin core structure helped to achieve the favorable orientation. All group 1 compounds adopted the canonical binding pose so that their 7-OH group pinpointed to the sulfone group of PAPS in the catalytic sites of SULTs 1A1, 1C4, and 1E1.

This study proved that the 7-hydroxycoumarin derivatives **9** and **11**, which were measured to have ~1 μM K_m-values and were modelled to acquire the canonical pose at the catalytic site, are selective substrates for human SULT1E1. Similarly, the SULT1A1 selective substrate **14** with a 0.91 μM K_m-value follows the same binding pattern. Several 7-hydroxycoumarins were sulfonated by two or three human SULTs such as 1A1, 1C4, or 1E1. All these compounds can be used as probe substrates to study estrogen sulfonating SULTs such as 1E1 and 1A1 instead of using estrogens. The benefit of using 7-hydroxycoumarin derivatives is that their sulfonation measurement is easier, faster and less expensive than sulfonation measurement of estrogens, because quantitative analysis of 7-hydroxycoumarin sulfonation is based on fluorescence instead of using LC-MS technology in estrogen sulfonation activity measurements (Kushida et al., 2011; Ledeck et al., 2022). 2-aryl substituted hydroxybenzothiazole derivatives have been developed to investigate sulfonation by human SULTs and selectively SULT1E1 (Cole et al., 2010). Measurement of these compounds was performed using (Korb et al., 2009) S-labelled PAPS, which transformed sulfonated compounds radioactive, the sulfated metabolites were separated on a thin layer chromatography plate, and the metabolite spots quantified in autography. p-Nitrophenol and 2-naphthol are old substrates (absorbance--based technology substrates) to measure SULT1A1 (Rohn et al., 2012; Falany et al., 1995).

Sulfonation by SULT1A1 or SULT1E1 can be determined using tissue samples or recombinant SULTs. When recombinant SULT enzymes are used, the selectivity of the substrate is not essential, as reactions by other SULTs do not occur. However, if tissue samples are used, the selectivity of the substrate gives more precise information about the studied reaction than non-selective substrates, as only one SULT sulfonates the selective 7-hydroxycoumarin derivatives such as **9** and **11** (SULT1E1) or **14** (SULT1A1), whereas several SULTs are involved in sulfonation of non-selective 7-hydroxycoumarin derivatives. Therefore, 7-hydroxycoumarins **9, 11**, and **14** would be better suited for studies with tissue samples than the other 7-hydroxycoumarins. Fluorescent 7-hydroxycoumarin and the previously described 1-aryl substituted hydroxybenzothiazole (Cole et al. 2010) probe substrates could be used to compare sulfonation rates between different samples such as animal species, tissues or recombinant SULTs, to study inhibition of sulfonation by old or new chemical entities and visualization of sulfonation in cellular compartments of different kinds of samples such as cell lines or tissues expressing SULTs.

5. Conclusions

1. Sulfonation rates and kinetic parameters were determined for 19 7-hydroxycoumarin derivatives with human SULTs 1A1, 1A2, 1A3, 1B1, 1C2, 1C4, 1E1, and 2A1 (Fig. 2–4; Fig S2 and S4, Tables S1-S2).
2. A thorough structural bioinformatics analysis (Fig. 2–4) was performed to determine the atomistic basis behind the sulfonation differences (Table S1) among the 7-hydroxycoumarin derivatives by the eight SULTs – these results are summarized in a SAR model in Fig. 7.
3. Estrogen mimetic derivatives **8**–**14** or C-3 aryl substituted 7-hydroxycoumarins were sulfonated by SULT1A1 and SULT1E1, which are estrogen sulfonating SULTs. Importantly, derivatives **9** and **11** were determined as selective substrates for SULT1E1 and **14** for SULT1A1.

4. Incorporation of 7-hydroxycoumarin derivatives **8**–**14** into a pre-reaction model of SULT1A1 and SULT1E1 generated good shape matches in the active sites explaining their high sulfonation rates (Fig. 5).
5. Because sulfonation of 7-hydroxycoumarin derivatives quench their fluorescence, these compounds can be used as quantitative probe compounds to study sulfonation of human SULTs and particularly the estrogen sulfonating SULT1E1 and SULT1A1. These measurements are faster, less expensive and easier than sulfonation measurements of estrogens with LC-MS technology. They can be applied to drug screening, inhibition testing, study of SULTs' catalytic mechanism and microscopical visualization studies using various sample types.

Human and animal rights and informed consent

This article does not contain any studies with human or animal subjects by any of the authors.

Funding

Novo Nordisk Foundation (O.T.P.; Pioneer Innovator Grant, grant number 0068,926; Distinguished Innovator Grant; grant number 0075,825) funded the research. This research was also supported by the Research Council of Finland's Flagship InFLAMES (P.A.P.). The funding decision numbers are 337,530 and 357,910. This work was supported by the National Institutes of Health (grant number: Z01ES1005–01) (MF).

Declaration of interests

The authors declare that they have no known competing financial interests or personal relationships that could have appeared to influence the work reported in this paper.

Declaration of generative AI and AI-assisted technologies in the writing process

The authors have not used AI and AI-assisted technologies in the writing process.

CRediT authorship contribution statement

Risto O. Juvonen: Writing – review & editing, Writing – original draft, Visualization, Validation, Supervision, Resources, Project administration, Methodology, Investigation, Formal analysis, Conceptualization. **Pekka A. Postila:** Writing – review & editing, Writing – original draft, Visualization, Validation, Methodology, Investigation, Formal analysis, Conceptualization. **Pankaj Kumar Singh:** Writing – review & editing, Methodology, Investigation, Formal analysis. **Juhani Huuskonen:** Writing – review & editing, Resources, Methodology. **Juri Timonen:** Writing – review & editing, Resources, Methodology. **Muluneh Fashe:** Writing – review & editing, Resources, Methodology. **Rasikh Hussain:** Writing – review & editing, Methodology, Investigation, Formal analysis. **Zaeema Aqip:** Writing – review & editing, Methodology, Investigation, Formal analysis. **Olli Kärkkäinen:** Writing – review & editing, Methodology, Investigation, Formal analysis. **Hannu Raunio:** Writing – review & editing, Visualization, Resources, Project administration, Conceptualization. **Olli T. Pentikäinen:** Writing – review & editing, Visualization, Resources, Project administration, Methodology, Investigation, Formal analysis, Conceptualization.

Declaration of competing interest

The authors declare the following financial interests/personal relationships which may be considered as potential competing interests:

I and my coauthors have nothing to decleare If there are other authors, they declare that they have no known competing financial interests or personal relationships that could have appeared to influence the work reported in this paper.

Acknowledgements

The authors wish to acknowledge Ms. Hannele Jaatinen for technical help, Biocenter Finland/DDCB for financial support. The Finnish IT Center for Science (CSC) is acknowledged for generous computational resources (O.T.P.: Project Nos. jyy2516 and jyy2585; P.A.P.: Project No. tty3975), and the Turku Screening Unit of the Drug Discovery and Chemical Biology platform of Biocentre Finland is acknowledged for support.

Supplementary materials

Supplementary material associated with this article can be found, in the online version, at doi:10.1016/j.ejps.2025.107249.

Data availability

Data will be available on request.

References

Alcolombri, U., Elias, M., Tawfik, D.S., 2011. Directed evolution of sulfotransferases and paraoxonases by ancestral libraries. J. Mol. Biol. 411, 837–853.

Allali-Hassani, A., Pan, P.W., Dombrovski, L., Najmanovich, R., Tempel, W., Dong, A., Loppnau, P., Martin, F., Thonton, J., Edwards, A.M., Bochkarev, A., Plotnikov, A.N., Vedadi, M., Arrowsmith, C.H., 2007. Structural and chemical profiling of the human cytosolic sulfotransferases. PLoS. Biol. 5, 1063–1078.

Amenyogbe, E., Chen, G., Wang, Z., Lu, X., Lin, M., Lin, A.Y., 2020a. A review on sex steroid hormone estrogen receptors in mammals and fish. Int. J. Endocrinol. vol. 2020. https://doi.org/10.1155/2020/5386193. Preprint at.

Amenyogbe, E., Chen, G., Wang, Z., Lu, X., Lin, M. & Lin, A.Y. A review on sex steroid hormone estrogen receptors in mammals and fish. (2020) doi:10.1155/2020/5386193.

Berger, I., Guttman, C., Amar, D., Zarivach, R., Aharoni, A., 2011a. The molecular basis for the broad substrate specificity of human sulfotransferase 1A1. PLoS. One 6.

Berger, I., Guttman, C., Amar, D., Zarivach, R., Aharoni, A., 2011b. The molecular basis for the broad substrate specificity of Human sulfotransferase 1A1. PLoS. One 6, e26794.

Berman, H.M., Westbrook, J., Feng, Z., Gilliland, G., Bhat, T.N., Weissig, H., Shindyalov, I.N., Bourne, P.E., 2000. The Protein Data Bank. Nucleic. Acids. Res. vol. 28. http://www.rcsb.org/pdb/status.html.

Blanchard, R.L., Freimuth, R.R., Buck, J., Weinshilboum, R.M., Coughtrie, M.W.H., 2004. A Proposed Nomenclature System for the Cytosolic Sulfotransferase (SULT) Superfamily, 14. Lippincott Williams & Wilkins Pharmacogenetics, pp. 199–211.

Cole, G.B., Keum, G., Liu, J., Small, G.W., Satyamurthy, N., Kepe, V., Barrio, J.R., 2010. Specific estrogen sulfotransferase (SULT1E1) substrates and molecular imaging probe candidates. Proc. Natl. Acad. Sci. u S. a 107, 6222–6227.

Coughtrie, M.W.H, 2016. Function and organization of the human cytosolic sulfotransferase (SULT) family. Chem. Biol. Interact. 259, 2–7.

Falany, C.N., Krasnykh, V., Falany, J.L., 1995. Bacterial expression and characterization of a cDNA for human liver estrogen sulfotransferase. J. Steroid. Biochem. Mol. Biol. 52, 529–539.

Gamage, N.U., Duggleby, R.G., Barnett, A.C., Tresillian, M., Latham, C.F., Liyou, N.E., McManus, M.E., Martin, J.L., 2003a. Structure of a human carcinogen-converting enzyme, SULT1A1. Structural and kinetic implications of substrate inhibition. J. Biol. Chem. 278, 7655–7662.

Gamage, N.U., Duggleby, R.G., Barnett, A.C., Tresillian, M., Latham, C.F., Liyou, N.E., McManus, M.E., Martin, J.L., 2003b. Structure of a Human carcinogen-converting enzyme, SULT1A1. J. Biol. Chem. 278, 7655–7662.

Gamage, N.U., Tsvetanov, S., Duggleby, R.G., McManus, M.E., Martin, J.L., 2005a. The structure of Human SULT1A1 crystallized with estradiol: an insight into active site plasticity and substrate inhibition with multi-ring substrates. J. Biol. Chem. 280, 41482–41486.

Gamage, N.U., Tsvetanov, S., Duggleby, R.G., McManus, M.E., Martin, J.L., 2005b. The structure of Human SULT1A1 crystallized with Estradiol. J. Biol. Chem. 280, 41482–41486.

Gibson, D.A., Simitsidellis, I., Collins, F., Saunders, P.T.K., 2020a. Androgens, oestrogens and endometrium: a fine balance between perfection and pathology. J. Endocrinol. vol. 246, R75–R93. https://doi.org/10.1530/JOE-20-0106. Preprint at.

Gibson, D.A., Simitsidellis, I., Collins, F., Saunders, P.T.K., 2020b. Androgens, oestrogens and endometrium: a fine balance between perfection and pathology. J. Endocrinol. 246, R75–R93.

Gosavi, R.A., Knudsen, G.A., Birnbaum, L.S., Pedersen, L.C., 2013. Mimicking of estradiol binding by flame retardants and their metabolites: a crystallographic analysis. Environ. Health Perspect. 121, 1194–1199.

Isaacs, C., Wellstein, A., Riegel, A.T., 2017. Hormones and related agents in the therapy of cancer. In: Brunton, L.L., Hilal-Dandan, R., Knollmann, B.C. (Eds.), Goodman & Gilman's: The Pharmacological Basis of Therapeutics, 13e. McGraw-Hill Education.

Jacobson, M.P., Pincus, D.L., Rapp, C.S., Day, T.J.F., Honig, B., Shaw, D.E., Friesner, R. A., 2004. A hierarchical approach to all-atom protein loop prediction. Proteins: Struc., Function Genetics 55, 351–367.

Jiang, M., Klein, M., Zanger, U.M., Mohammad, M.K., Cave, M.C., Gaikwad, N.W., Dias, N.J., Selcer, K.W., Guo, Y., He, J., Zhang, X., Shen, Q., Qin, W., Li, J., Li, S., Xie, W., 2016. Inflammatory regulation of steroid sulfatase: a novel mechanism to control estrogen homeostasis and inflammation in chronic liver disease. J. Hepatol. 64, 44–52.

Jumper, J., Evans, R., Pritzel, A., Green, T., Figurnov, M., Ronneberger, O., Tunyasuvunakool, K., Bates, R., Žídek, A., Potapenko, A., Bridgland, A., Meyer, C., Kohl, S.A.A., Ballard, A.J., Cowie, A., Romera-Paredes, B., Nikolov, S., Jain, R., Adler, J., Back, T., Petersen, S., Reiman, D., Clancy, E., Zielinski, M., Steinegger, M., Pacholska, M., Berghammer, T., Bodenstein, S., Silver, D., Vinyals, O., Senior, A.W., Kavukcuoglu, K., Kohli, P., Hassabis, D., 2021. Highly accurate protein structure prediction with AlphaFold. Nature 2021 596:7873 596, 583–589.

Juvonen, R.O., Rauhamäki, S., Kortet, S., Niinivehmas, S., Troberg, J., Petsalo, A., Huuskonen, J., Raunio, H., Finel, M., Pentikäinen, O.T., 2018. Molecular docking-based design and development of a highly selective probe substrate for UDP-glucuronosyltransferase 1A10. Mol. Pharm. 15.

Juvonen, R.O., Pentikäinen, O., Huuskonen, J., Timonen, J., Kärkkäinen, O., Heikkinen, A., Fashe, M., Raunio, H., 2020. In vitro sulfonation of 7-hydroxycoumarin derivatives in liver cytosol of human and six animal species. Xenobiotica 50.

Korb, O., Stützle, T., Exner, T.E., 2009. Empirical scoring functions for advanced protein-Ligand docking with PLANTS. J. Chem. Inf. Model. 49, 84–96.

Kushida, A., Hattori, K., Yamaguchi, N., Kobayashi, T., Date, A., Tamura, H., 2011. Sulfation of estradiol in Human epidermal keratinocyte. Biol. Pharm. Bull. 34, 1147–1151.

Ledeck, J., Dufour, P., Evrard, É., Le Goff, C., Peeters, S., Brutinel, F., Egyptien, S., Deleuze, S., Cavalier, É., Ponthier, J., 2022. Evolution of 17-β-estradiol, estrone and estrone-sulfate concentrations in late pregnancy of different breeds of mares using Liquid Chromatography and Mass Spectrometry. Theriogenology 189, 86–91.

Lehtonen, J.V., Still, D.-J., Rantanen, V.-V., Ekholm, J., Björklund, D., Iftikhar, Z., Huhtala, M., Repo, S., Jussila, A., Jaakkola, J., Pentikäinen, O., Nyrönen, T., Salminen, T., Gyllenberg, M., Johnson, M.S., 2004. BODIL: A molecular modeling environment for structure-function analysis and drug design. J. Comput. Aided. Mol. Des. 18.

Leow, J.W.H., Chan, E.C.Y., 2019. Atypical Michaelis-Menten kinetics in cytochrome P450 enzymes: a focus on substrate inhibition. Biochem. Pharmacol. 169.

Levin, E.R., Vitek, W.S., Hammes, S.R., 2017. Estrogens, progestins, and the female reproductive tract. In: Brunton, L.L., Hilal-Dandan, R., Knollmann, B.C. (Eds.), Goodman & Gilman's: The Pharmacological Basis of Therapeutics, 13e. McGraw-Hill Education.

Lu, C., Wu, C., Ghoreishi, D., Chen, W., Wang, L., Damm, W., Ross, G.A., Dahlgren, M.K., Russell, E., Von Bargen, C.D., Abel, R., Friesner, R.A., Harder, E.D., 2021. OPLS4: improving force field accuracy on challenging regimes of chemical space. J. Chem. Theory. Comput. 17, 4291–4300.

Niinivehmas, S., Pentikäinen, O.T., 2021. Coumarins as tool compounds to aid the discovery of selective function modulators of steroid hormone binding proteins. Molecules. 26.

Niinivehmas, S.P., Manivannan, E., Rauhamäki, S., Huuskonen, J., Pentikäinen, O.T., 2016. Identification of estrogen receptor α ligands with virtual screening techniques. J. Mol. Graph. Model. 64.

Niinivehmas, S., Postila, P.A., Rauhamäki, S., Manivannan, E., Kortet, S., Ahinko, M., Huuskonen, P., Nyberg, N., Koskimies, P., Lätti, S., Multamäki, E., Juvonen, R.O., Raunio, H., Pasanen, M., Huuskonen, J., Pentikäinen, O.T., 2018. Blocking oestradiol synthesis pathways with potent and selective coumarin derivatives. J. Enzyme Inhib. Med. Chem. 33.

Nishiyama, T., Ogura, K., Kaku, T., Takahashi, E., Ohkubo, Y., Sekine, K., Hiratsuka, A., Watabe, T., Nakano, H., Kadota, S., 2002. Sulfation of environmental estrogens by cytosolic human sulfotransferases. Drug Metab. Pharmacokinet. 17, 221–228.

Parkinson, A., Ogilvie, B.W., Buckley, D.B., Kazmi, F., Czerwinski, M., Parkinson, O., 2019. Biotransformation of xenobiotics. In: Klaassen, C.D. (Ed.), Casarett & Doull's Toxicology: The Basic Science of Poisons, 9th ed. Mc Graw Hill, pp. 119–430.

Pedersen, L.C., Petrotchenko, E., Shevtsov, S., Negishi, M., 2002. Crystal structure of the Human estrogen sulfotransferase-PAPS complex: evidence for catalytic role of ser137 in the sulfuryl transfer reaction. J. Biol. Chem. 277, 17928–17932.

Reed, M.J., Purohit, A., Woo, L.W.L., Newman, S.P., Potter, B.V.L., 2005. Steroid sulfatase: molecular biology, regulation, and inhibition. Endocr. Rev. vol. 26, 171–202. https://doi.org/10.1210/er.2004-0003. Preprint at.

Rohn, K.J., Cook, I.T., Leyh, T.S., Kadlubar, S.A., Falany, C.N., 2012. Potent inhibition of human sulfotransferase 1A1 by 17α-ethinylestradiol: role of 3'-phosphoadenosine 5'-phosphosulfate binding and structural rearrangements in regulating inhibition and activity. Drug Metab. Dispos. 40, 1588–1595.

Sagawa, N., Shikata, T., 2014. Hydration numbers of nitro compounds and nitriles in aqueous solution. Phys. Chem. Chem. Phys. 16, 13262–13270.

Shelley, J.C., Cholleti, A., Frye, L.L., Greenwood, J.R., Timlin, M.R., Uchimaya, M., 2007. Epik: a software program for pKa prediction and protonation state generation for drug-like molecules. J. Comput. Aided. Mol. Des. 21, 681–691.

Shevtsov, S., Petrochenko, E.V., Pedersen, L.C., Negishi, M., 2003. Crystallographic analysis of a hydroxylated polychlorinated biphenyl (OH-PCB) bound to the catalytic estrogen binding site of human estrogen sulfotransferase. Environ. Health Perspect. 111, 884–888.

Squirewell, E.J., Duffel, M.W., 2015. The effects of endoxifen and other major metabolites of tamoxifen on the sulfation of estradiol catalyzed by human cytosolic sulfotransferases hSULT1E1 and hSULT1A1×1. Drug Metab. Dispos. 43, 843–850.

Testa, B., Krämer, S.D., 2008. The biochemistry of drug metabolism - an introduction: part 4. Reactions of conjugation and their enzymes. Chem. Biodiver. vol. 5, 2171–2336. https://doi.org/10.1002/cbdv.200890199. Preprint at.

Thomas, M.P., Potter, B.V.L., 2013. The structural biology of oestrogen metabolism. J. Steroid Biochem. Molec. Biol. vol. 137, 27–49. https://doi.org/10.1016/j.jsbmb.2012.12.014. Preprint at.

Timonen, J.M., Nieminen, R.M., Sareila, O., Goulas, A., Moilanen, L.J., Haukka, M., Vainiotalo, P., Moilanen, E., Aulaskari, P.H., 2011. Synthesis and anti-inflammatory effects of a series of novel 7-hydroxycoumarin derivatives. Eur. J. Med. Chem. 46, 3845–3850.

Yi, M., Negishi, M., Lee, S.J., 2021a. Estrogen sulfotransferase (SULT1E1): its molecular regulation, polymorphisms, and clinical perspectives. J. Pers. Med. vol. 11. https://doi.org/10.3390/jpm11030194. Preprint at.

Yi, M., Negishi, M., Lee, S.J., 2021b. Estrogen sulfotransferase (SULT1E1): its molecular regulation, polymorphisms, and clinical perspectives. J. Pers. Med. 11.

Zhang, H., Varmalova, O., Vargas, F.M., Falany, C.N., Leyh, T.S., 1998. Sulfuryl transfer: the catalytic mechanism of human estrogen sulfotransferase. J. Biol. Chem. 273, 10888–10892.